

Micro-surface and bulk thermal behavior of a single-grain decagonal Al–Ni–Co quasicrystal

Jack A. Barrow^{a,d}, Melbourne C. Lemieux^e, Bruce A. Cook^{b,e}, Amy R. Ross^{b,e},
Vladimir V. Tsukruk^e, Paul C. Canfield^{c,f}, Daniel J. Sordelet^{b,e,*}

^a *Materials Chemistry Program, Ames Laboratory, Ames, IA 50011, USA*

^b *Metal and Ceramic Sciences Program, Ames Laboratory, Ames, IA 50011, USA*

^c *Condensed Matter Physics Program, Ames Laboratory, Ames, IA 50011, USA*

^d *Department of Chemistry, Iowa State University, Ames, IA 50011, USA*

^e *Department of Materials Science and Engineering, Iowa State University, Ames, IA 50011, USA*

^f *Department of Physics and Astronomy, Iowa State University, Ames, IA 50011, USA*

Abstract

Scanning thermal microscopy is used to examine the thermal behavior of specific surfaces of a ~ 0.8 cm³ single-grain Al₇₄Ni₁₀Co₁₆ decagonal quasicrystal. The response of a micro-thermal probe in contact with aperiodic and periodic surfaces in air reveals the anisotropic heat flow of the decagonal structure. Heat dissipation with the probe on the aperiodic surface is higher than when the probe is on the periodic surface. While the SThM technique is generally considered to be constrained to the surface region below the nominally 2–5 μ m probe tip radius, the heat flow data obtained are clearly comprised of contributions from both the lateral surface around the probe tip and a volume normal to the surface in contact. Heat flow in the decagonal Al₇₄Ni₁₀Co₁₆ quasicrystal can be modeled by an elliptical distribution of thermal diffusion. Parameters for the model used in this study were obtained by making bulk thermal diffusivity measurements using the laser flash method on specimens along the 2- and 10-fold directions. The model was applied to a surface oriented 45° to the major axes and verified from bulk measurements obtained from a sample cut along this orientation.

© 2004 Elsevier B.V. All rights reserved.

PACS: 61.44.Br; 64.70.Kb; 61.10.Nz; 81.05.Kf

1. Introduction

Thermal transport in quasicrystals is well known to be anomalously low compared to intermetallic phases; moreover, the dependence of thermal diffusivity on temperature and sample purity is unique to quasicrystals. For example, icosahedral Al–Cu–Fe shows an isotropic thermal conductivity around 2.0 W m⁻¹ K⁻¹ at 273 K that increases to near 8 W m⁻¹ K⁻¹ at 1000 K [1]. Decagonal quasicrystals, which are constructed of a periodic stacking of planes having aperiodic 10-fold rotational symmetry, exhibit highly anisotropic behavior. Single grains of Al–Ni–Co decagonal quasicrystals

have been used to determine thermal conductivities along aperiodic and periodic directions [2,3]. Most thermal transport studies, however, have focused on temperatures at and far below 300 K. In addition, the conventional thermal transport measurement techniques used with decagonal quasicrystals interrogate the entire bulk of the sample; near-surface effects are not separable.

To investigate the thermal transport behavior of aperiodic and periodic surfaces, a relatively new technique referred to as scanning thermal microscopy (SThM) is being utilized. This method is a derivative of the scanning probe microscopy family and is conceptually very similar to atomic force microscopy (AFM). With SThM a miniature thermal probe (tip radius ~ 2 – 5 μ m) replaces the cantilevered tip in AFM and is utilized to collect simultaneous information about the localized heat dissipation and surface topography at the point of physical contact between the probe tip and the surface.

* Corresponding author. Tel.: +1-515 294 4713; fax: +1-515 294 8727.

E-mail address: sordelet@ameslab.gov (D.J. Sordelet).

Because of the comparatively large tip size, the spatial resolution of surface topography is lower than with conventional (AFM). As reported by Gorbunov et al., the spatial resolution of the surface distribution of thermal response is around 1 and 0.1 μm for compliant and hard surfaces, respectively [4,5]. In an alternate configuration using a reference probe, differential microthermal analysis may be performed up to 725 K. The general thermal probe and sample orientations are described in Refs. [4–7].

The objective of an ongoing program in our lab is to examine and distinguish between the thermal behavior of aperiodic and periodic surfaces in a decagonal $\text{Al}_{74}\text{Ni}_{10}\text{Co}_{16}$ quasicrystal. Experimental details and initial results compared to recently obtained bulk thermal properties from the same quasicrystal sample are presented here.

2. Experimental procedures

A large (0.8 cm^3) single-grain decagonal $\text{Al}_{74}\text{Ni}_{10}\text{Co}_{16}$ quasicrystal was grown using the flux growth technique [8]. The sample has a rod-like morphology, with the c -axis parallel to the length of the rod and 10-side growth facets oriented normal to the c -axis, reflecting the decagonal symmetry of the quasicrystal structure. Spark erosion was used to cut samples for the SThM experiments. Samples with parallel faces of approximately 1 cm^2 in area and 0.2 cm in thickness were ground and mechanically polished to a roughness of 0.1–0.5 nm, as measured with tapping mode AFM. As shown schematically in Fig. 1, the aperiodic and periodic sample surfaces are perpendicular to the periodic c -axis and the aperiodic radial axes, respectively. Pieces of the remaining single-grain adjacent to the harvested samples were cut and crushed into powder for X-ray analysis. The structural quality of the sample used in this study is comparable, based on powder X-ray diffraction data, to the sample having the same nominal composition described in Ref. [8].

Initially, the SThM measurements were performed in a thermal mapping mode where the probe is scanned across the sample surface, as in normal AFM techniques. The probe is kept at a constant temperature and heat dissipation is monitored to obtain a landscape of thermal conductivity contrast over the area scanned, which is typically about $5 \times 5 \mu\text{m}^2$ to $100 \times 100 \mu\text{m}^2$. During thermal mapping, topographical information from the surface is also recorded as the tip position is monitored. Subsequently, a micro-thermal analysis mode was used to measure localized heat dissipation of a particular surface with the probe tip held stationary at tip temperatures up to 525 K.

Following the SThM experiments, bulk thermal diffusivity measurements were performed using the laser



Fig. 1. Schematic drawing of a decagonal quasicrystal to illustrate orientation of samples machined for SThM and bulk thermal measurements.

flash method on similar specimens that were harvested from the original single-grain sample, as depicted in Fig. 1. One face of a sample was irradiated with a 628 nm laser using a 1 ms pulse. The resulting thermal transient was measured as a function of time on the opposite surface using a liquid nitrogen cooled InSb infrared detector. Further details are discussed elsewhere [9]. In this configuration, irradiating the aperiodic and periodic surfaces provides bulk thermal diffusivity data along the 2-fold and 10-fold directions, respectively. Additionally, the same measurements were performed on the sample having faces oriented at 45° from the major axes: see the middle portion of Fig. 1. To calculate thermal conductivity values from the thermal diffusivity results, the density was measured by the Archimedes technique to be 4.01 g/cm^3 , and the temperature-dependent heat capacity, measured in a Perkin Elmer Pyris 7 DSC, ranged from 22 to 65 $\text{J mol}^{-1} \text{K}^{-1}$ between 325 and 900 K. The thermal conductivity was then determined from the product of the thermal diffusivity, density, and heat capacity.

3. Results

Characteristic surface topography and heat dissipation maps from aperiodic and periodic surfaces at 323 K are presented in Fig. 2. The surface roughness measured from multiple samples ranged between 0.1 and 0.5 nm. Based on previous work with other materials, this roughness is adequate to ensure constant probe tip contact area during SThM (i.e., heat dissipation is not influenced by geometrical contributions) [4,5]. The thermal maps obtained from $80 \times 80 \mu\text{m}^2$ areas illustrate two features. First, good agreement exists between the

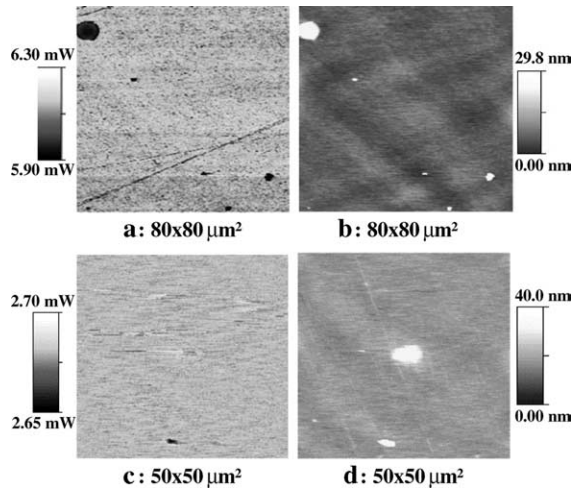


Fig. 2. Thermal maps ($50 \times 50 \mu\text{m}$) of (a) aperiodic and (b) periodic surfaces and corresponding topography profiles for (c) aperiodic and (d) periodic surfaces obtained at 325 K using SThM. Insets display maximum and minimum heat dissipation and surface height measured over each surface.

heat dissipation and topography data. For example, foreign debris is visible on the thermal map of the aperiodic surface (Fig. 2(a)) and appears on the corresponding topography map (Fig. 2(c)). This debris clearly has different thermal properties from the quasicrystal sample. Second, with the thermal probe scanning over the aperiodic surface, the range of total heat dissipation is larger than under the same conditions with the probe scanning the periodic surface (see insets in Fig. 2(a) and (b)). This latter observation illustrates the resolution capability of this SThM technique to distinguish between these two surfaces having different thermal transport characteristics.

Similar experimental SThM evidence for higher heat flow at the aperiodic surface was observed in a micro-thermal analysis made as a function of temperature. Fig. 3 shows the variation in heat dissipation at the probe–surface contact point at different temperatures for both surfaces. Again, higher heat dissipation was measured while keeping the probe at constant temperature and in contact with the aperiodic surface. Heat dissipation measured by the same micro-thermal analysis technique from a polycrystalline alumina, which has a higher thermal conductivity than typical quasicrystals, is displayed for comparison [1]. Although not shown here, similar surface-dependent heat flow was measured in a micro-differential scanning calorimetry analysis mode.

The bulk thermal diffusivity data obtained along the 2-fold and 10-fold directions are shown in Fig. 4. A clear anisotropy is visible, with the expected higher thermal transport along the periodic, 2-fold direction (i.e., axis perpendicular to the aperiodic face outlined in Fig. 1). This is consistent with the anisotropy observed in the SThM experiments described above. When diffusivity is

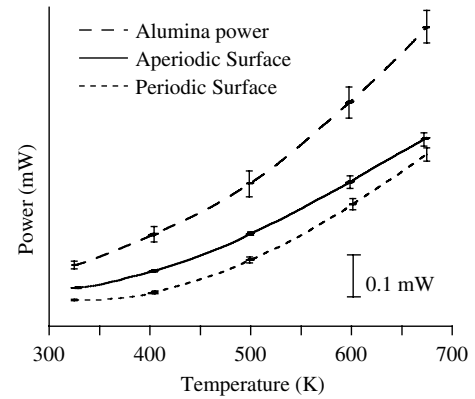


Fig. 3. Average micro-thermal analysis heat dissipation data measured with the SThM thermal probe applied perpendicular to the aperiodic surface (i.e., parallel to the 10-fold axis) and applied perpendicular to the periodic surface (i.e., parallel to a 2-fold axis) at different temperatures. Heat dissipation measured from a polycrystalline alumina sample is shown for comparison.

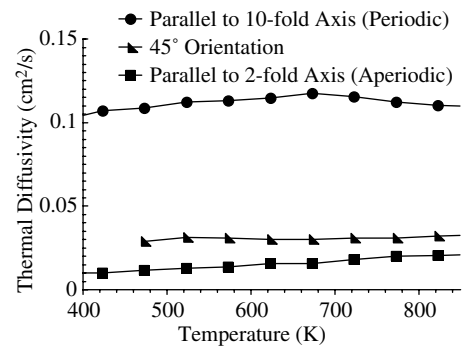


Fig. 4. Bulk thermal diffusivity data collected parallel to the 10- and 2-fold axes and along a sample oriented at 45° to the major axes. The standard deviation of each data point is less than 0.007, 0.0009, and 0.003 for measurements made parallel to the 10-fold, 2-fold, and 45° axes, respectively.

used to deduce thermal conductivity, these results along the primary directions appear to be a continuation of the lower temperature conductivity values measured by Zhang et al. using an Al–Ni–Co decagonal quasicrystal [2]. At 300 K, they report thermal conductivities of 16 and $2.5 \text{ W m}^{-1} \text{ K}^{-1}$ along the 2-fold and 10-fold directions, respectively. Thermal diffusivity values measured from the sample having faces oriented 45° to the major axes are between the results from the other two directions. A suggestion for why the thermal diffusivity through the 45° off-axis direction is closer to that of the aperiodic, 10-fold direction is presented below.

4. Discussion

Low temperature measurements reported by Zhang and Matsukawa, show that thermal conductivity in

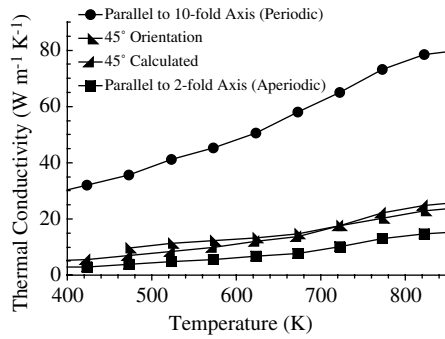


Fig. 5. Bulk thermal conductivity values parallel to the 10- and 2-fold axes and along a sample oriented at 45° to the major axes. Included are values calculated from the elliptical thermal diffusion model discussed in the text. The propagated standard deviation for each data point is less than 3, 0.4, and 0.9 for measurements made parallel to the 10-fold, 2-fold and 45° axes, respectively.

decagonal quasicrystals is higher along the periodic axis [2,3]. Our measurements of thermal conductivity demonstrate that this trend continues to higher temperatures. The SThM experiments are also consistent with this trend, although it is noted that the ratio of heat flow measured between the two surfaces with SThM (Fig. 3) is much lower than that seen in the thermal conductivity shown in Fig. 5. The lower anisotropy in the SThM measurements suggest that the SThM measurements made in this study comprise heat flow contributions from the lateral region of a specific surface surrounding the thermal probe, as well as from the bulk (i.e., contributions to overall heat flow arise from components of the two major axes).

To understand aperiodic and periodic directional thermal transport contributions, which are considered to be vector quantities corresponding to principal axes, it is necessary to resolve them individually. To do this, we use the thermal ellipsoid model, first described by Voigt [10]. This model has been used by Bridgman to explain anisotropic conductivity in metallic single crystals [11]. The ellipsoidal boundary of our isothermal may be represented by Eq. (1).

$$\frac{x^2}{r^2 K_a} + \frac{y^2}{r^2 K_p} = \frac{1}{K_\theta} \quad (1)$$

K_p is the periodic axis of thermal conductivity. This axis is coincident with the 10-fold symmetry axis. K_a is the aperiodic axis of thermal conductivity, which is coincident with the 2-fold symmetry axis. x and y are the coordinates at which the heat flux vector r , intersects the isotherm. K_θ is the thermal conductivity in the direction of vector r .

The direction of vector r may also be described in terms of θ , the angle of r measured relative to the 10-fold symmetry axis. Eq. (1) may be written in terms of θ , by using $\cos \theta = \frac{y}{r}$ and $\sin \theta = \frac{x}{r}$ to transform to a polar coordinate system. This is shown, simplified, as Eq. (2).

$$K_\theta = \left[\frac{1}{K_a} + \left(\frac{1}{K_p} - \frac{1}{K_a} \right) \cos^2 \theta \right]^{-1} \quad (2)$$

Solutions for K_θ are generated using experimentally determined values of K_a and K_p at given temperatures. Solutions are calculated for $\theta = 45^\circ$ over the measured temperature range and compared to experimental data for a decagonal $\text{Al}_{74}\text{Ni}_{10}\text{Co}_{16}$ sample cut with a 45° normal axis.

Fig. 5 shows the bulk thermal conductivity values of the $\text{Al}_{74}\text{Ni}_{10}\text{Co}_{16}$ decagonal quasicrystal along the two primary axes and along an axis oriented at 45°. Also shown is the calculated thermal conductivity for $\theta = 45^\circ$ based on the thermal ellipsoid model. The prediction agrees reasonably well with the measured data. Notice that it appears that K_p does not contribute to K_θ as significantly as K_a . This is a consequence of the anisotropic heat flow. For $\theta = 45^\circ$, the flux vector intersecting the isotherm contains a higher percentage of the total aperiodic flux vector than of the periodic flux vector. In fact, by the thermal ellipsoid model we would not expect an equal periodic and aperiodic flux contribution until $\theta \approx 21^\circ$. This is why the conductivity values along the 45° axis are skewed towards those values measured along the 2-fold axis.

5. Conclusions

The thermal behavior of a large, single-grain $\text{Al}_{74}\text{Ni}_{10}\text{Co}_{16}$ decagonal quasicrystal was examined using scanning thermal microscopy at temperatures between 325 and 725 K. Heat dissipation was measured with the thermal probe tip in contact with an aperiodic surface (i.e., surface normal to the 2-fold axis) and a periodic surface (i.e., surface normal to a 10-fold axis). Anisotropic heat flow was observed, with higher heat dissipation with the probe on the aperiodic surface. Thermal transport properties were also investigated using bulk diffusivity, heat capacity and density measurements to calculate thermal conductivity. Again, anisotropic heat flow was observed, with the higher heat flow occurring perpendicular to the aperiodic surface. The SThM measurements show a lower extent of anisotropy, indicating that heat flow in these experiments is not limited to the lateral surface surrounding the thermal probe, but also extends into a volume within the bulk normal to the surface. Thermal conductivity measurements were analyzed using an ellipsoidal thermal diffusion volume to describe the anisotropic heat flow. Bulk conductivity measurements along the principal axes were used to predict the conductivity through a surface oriented 45° to the major axes. Bulk measurements obtained from a sample cut along this orientation show good agreement with the values predicted using the thermal ellipsoid model.

Acknowledgements

This was supported by the United States Department of Energy (USDOE), Office of Science (OS), Office of Basic Energy Sciences (BES), through Iowa State University under Contract W-7405-ENG-82.

References

- [1] P. Archambault, C. Janot, *MRS Bull.* 22 (1997) 48.
- [2] D. Zhang, S. Cao, Y. Wang, L. Lu, X. Wang, X.L. Ma, K.H. Kuo, *Phys. Rev. Lett.* 66 (1991) 2778.
- [3] M. Matsukawa, M. Yoshizawa, K. Noto, Y. Yokoyama, A. Inoue, *Physica B (Amsterdam)* 263–264 (1999) 146.
- [4] V.V. Gorbunov, N. Fuchigami, J.L. Hazel, V.V. Tsukruk, *Langmuir* 15 (1999) 8340.
- [5] V.V. Gorbunov, N. Fuchigami, V.V. Tsukruk, *Probe Microsc.* 2 (2000) 53.
- [6] A. Majumdar, J.P. Carrero, J. Lai, *Appl. Phys. Lett.* 62 (1993) 2501.
- [7] A. Hammice, H.M. Pollock, M. Song, D. Hourston, *Measur. Sci. Technol.* 7 (1996) 142.
- [8] I.R. Fisher, M.J. Kramer, Z. Islam, A.R. Ross, A. Kracher, T. Wiener, M.J. Sailer, A.I. Goldman, P.C. Canfield, *Philos. Mag. B* 79 (1999) 425.
- [9] B.A. Cook, J.L. Harringa, C.B. Vining, *J. Appl. Phys.* 83 (1998) 5858.
- [10] W. Voigt, *Lehrbuch der Kristallphysik*, B.G. Teubner, Berlin, 1928 (Chapter VI).
- [11] P.W. Bridgman, *Proc. Am. Acad. Arts Sci.* 61 (1925) 101.